# A theoretical and experimental investigation of an in-band pumped gain-switched thulium-doped fiber laser*

Zhou Ren-Lai(周仁来)†, Ju You-Lun(鞠有伦), Zhao Jie(赵 杰), Yang Chao(杨 超), and Wang Yue-Zhu(王月珠)

*National Key Laboratory of Tunable Laser Technology, Harbin Institute of Technology, Harbin* 150001, *China*

(Received 11 October 2012; revised manuscript received 16 January 2013)

In this paper, the theoretical rate equation model of an in-band pumped gain-switched thulium-doped fiber (TDF) laser is investigated. The analytical formulations of pump energy threshold, peak power extraction efficiency, and pulse extraction efficiency are derived through analyzing the interaction process between the pump pulse and the laser pulse. They are useful for understanding, designing, and optimizing the in-band pumped TDF lasers in a 1.9 μm–2.1 μm wavelength region. The experiment with an all-fiber gain-switched TDF laser pumped by a 1.558-μm pulse amplifier is conducted, and our experimental results show good agreement with theoretical analysis.

**Keywords:** pulse fiber laser, gain-switched laser, thulium-doped fiber (TDF) laser, rate equation model, laser theory

**PACS:** 42.55.Ah, 42.55.Wd, 42.60.Mi **DOI:** 10.1088/1674-1056/22/6/064208

## 1. Introduction

Short pulse, high repetition rate laser sources emitting in a 1.9-μm∼2.1-μm spectral region have attracted much attention due to their various applications such as medical applications[1–4] and lidar for wind shear detection radar, remote sensing, atmospheric pollution monitoring, and range finders.[5,6] Additionally, high power 1.9 μm∼2.1 μm pulse lasers are efficient pump sources which can generate crucial mid-infrared countermeasure light sources by nonlinear frequency conversion technology. Commonly, a pulsed 1.9 μm–2.1 μm laser output can be directly achieved using $Tm^{3+}$-doped, $Ho^{3+}$-doped, or $Tm^{3+}$, $Ho^{3+}$ co-doped crystal (or ceramic) pumped by a laser diode, with up to 101-W in-band dual-end-pumped Q-switched Ho:YAG laser at 30 kHz serving as the highest output power pulse Ho laser as reported by Shen *et al.*[7] However, at high power levels, solid-state pulsed 1.9-μm∼2.1-μm laser outputs have not been successfully achieved due to the thermal lens effect or thermal damage to the laser crystal, and more complex laser geometries have to be adopted to compensate for thermally induced distortions which seriously reduce the efficiency of the laser.[8–11] Furthermore, the size and weight of the laser are always large due to the complex laser structure and geometry. Thus, these important factors mentioned above seriously restrict the applications of such lasers. Compared with the solid-state lasers in a 1.9-μm∼2.1-μm region, the $Tm^{3+}$-doped fiber (TDF) laser has significant advantages, such as, good reliability, good beam quality, compact fabrication, wide tunable range, heat dissipation, high conversion efficiency, and operational cost. As a result, pulse output TDF lasers have been a very popular theme in recent years.

There are two methods to generate the 1.9-μm∼2.1-μm laser nanosecond pulses in an active fiber. One method is to Q-switch a $Tm^{3+}$-doped, $Ho^{3+}$-doped or $Tm^{3+}$, $Ho^{3+}$ co-doped fiber laser, which has a distinct advantage and efficient generation of pulses in a single stage with the desired parameters. However, in conventional Q-switched fiber lasers, the laser pulse durations are in a range of $> 100$ ns in TDF.[12–14] In $Tm^{3+}$, $Ho^{3+}$ co-doped fiber, the output pulse shape is very sensitive to the cavity alignment, average output power decreases, and the pulses start fluctuating in duration[14] when the cavity is slightly misaligned, which can be attributed to the mode-locking modulation in Q-switched fiber laser, so the instability of output pulses seriously restricts their applications. The other method is to gain-switch a $Tm^{3+}$-doped, or $Ho^{3+}$-doped fiber. According to the $Tm^{3+}$ energy level structure, the generation of a pulse laser can follow three pump schemes, i.e., $^3H_6 \rightarrow {}^3H_4$ pumped by a 790-nm laser, $^3H_6 \rightarrow {}^3H_5$ pumped by a 1064-nm laser, and $^3H_6 \rightarrow {}^3F_4$ pumped by a 1550-nm laser. However, the output pulses of gain-switched TDF laser pumped by a 790-nm laser or 1064-nm laser are a series of relaxation spikes[15–17] due to the cross-relaxation effect (CRE) and the excited-state absorption (ESA) mechanism. The gain-switched $Tm^{3+}$-doped fiber laser pumped by a 1550-nm laser belongs to an in-band pumping scheme, and the cross-relaxation effect and ESA effect do not appear. The population of the $^3F_4$ energy level can be built up nearly instantaneously following the pump pulse and the stable short

*Project supported by the National Natural Science Foundation of China (Grant Nos. 60878011 and 61078008) and the Program for New Century Excellent Talents in University, China (Grant No. NCET-10-0067).

†Corresponding author. E-mail: zrlhit@126.com

© 2013 Chinese Physical Society and IOP Publishing Ltd 

pulse laser can be obtained without any relaxation spike. Thus, it is an excellent method to generate an all fiber pulse laser in TDF. In 2007, Jiang *et al.* demonstrated the stable short pulse (10 ns) generation from a gain-switched Tm-doped fiber laser in 2-μm region for the first time, and over a kilowatt of peak power is obtained at 2.5 kHz.[18] In 2011, Nakagami *et al.*[19] reported that a Tm-doped fiber laser operates around 1.9 μm by bi-directional pumping with modulated 1.6-μm-band laser diodes and the maximum output pulse power is measured to 119 mW. However, they also reported that the width of the output pulse is up to 5 μs and the output spectrum of a fiber laser is of muti-wavelength.[19] In the same year, Nikita *et al.*[20] reported on a compact monolithic 2000-nm pulsed laser with a single spatial mode output, ∼1.5-ns pulse duration, 8-kW peak power, and > 200-mW average power at 20-kHz repetition rate presented a monolithic, robustly polarized thulium fiber laser which produces pulses each with a 25-ns duration and an energy of up to 35 μJ at 2044 nm, and the large repetition rate, pulse energy, and average power will enable efficient energy extraction from a large mode-area, polarization maintaining thulium fiber amplifier.[20] Ding *et al.*[21] presented a monolithic, robustly polarised thulium fiber laser which produces pulses each with a 25-ns duration and an energy of up to 35 μJ at 2044 nm, and the large repetition rate, pulse energy, and average power will enable efficient energy extraction from a large mode-area, polarization maintaining thulium fiber amplifier reported on a compact monolithic 2000-nm pulsed laser with a single spatial mode output, ∼1.5-ns pulse duration, 8-kW peak power, and > 200-mW average power at 20-kHz repetition rate.

In 2011, Wang *et al.*[22] reported for the first time on the theoretical model of gain-switched TDF lasers pumped by acousto-optic modulated 1.56-μm lasers, and investigated the effects of some laser parameters on laser output.[22] However, in the process of their numerical simulation, only some parameters were taken into consideration, the general expressions about the laser output characteristics were not given and the physical process was not discussed. In this paper, the pump pulse action and laser pulse generation processes are analyzed in detail, and the explicit expressions of pump energy threshold, peak power extraction efficiency, and pulse extraction efficiency are given. The experiment performance of all fiber gain-switched TDF laser pumped by two stages 1.558-μm pulse amplifier shows good agreement with experimental results.

## 2. Theoretical analysis and numerical simulations

The dynamic behavior of in-band pumped TDF laser can be described by a set of coupled rate equations within a reasonable accuracy. Theoretically, a simplified two-level rate model is built to investigate the temporal characteristics, which takes into account the Stark-energy level structure of the upper ($^3F_4$) and lower ($^3H_6$) laser manifolds. The rate equations are given by[23–25]

$$\frac{dN_1(t)}{dt} = -\frac{P(t)}{A_{cor}h\nu_p}\Gamma_p\sigma_p[f_{lp}N_1(t) - f_{up}N_2(t)] + \frac{c}{n_{cor}}\Gamma_s\sigma_s[f_{us}N_2(t) - f_{ls}N_1(t)]\Phi(t) + \frac{N_2(t)}{\tau_f}, \quad (1)$$

$$\frac{dN_2(t)}{dt} = \frac{P(t)}{A_{cor}h\nu_p}\Gamma_p\sigma_p[f_{lp}N_1(t) - f_{up}N_2(t)] - \frac{c}{n_{cor}}\Gamma_s\sigma_s[f_{us}N_2(t) - f_{ls}N_1(t)]\Phi(t) - \frac{N_2(t)}{\tau_f}, \quad (2)$$

$$N_1(t) + N_2(t) = N_0, \quad (3)$$

$$\frac{d\Phi(t)}{dt} = \frac{l_f c}{Ln_{cor}}\Gamma_s\sigma_s[f_{us}N_2(t) - f_{ls}N_1(t)]\Phi(t) + \frac{l_f}{L}A_{21}\zeta N_2(t) - \frac{\Phi(t)}{\tau_0}, \quad (4)$$

where, $N_0$ is the $Tm^{3+}$ ion concentration; $N_1$ and $N_2$, each as a function of time, are population densities of $^3H_6$ level and $^3F_4$ level, respectively; $\sigma_e$ and $\sigma_a$ are the stimulated emission cross section and absorption cross section of the laser transition; $\Phi$ is the cavity photon density; $f_{up}$ and $f_{lp}$ are the Boltzmann factors of the upper and lower pump levels respectively; $f_{us}$ and $f_{ls}$ are the Boltzmann factors of the upper and lower laser levels respectively; $\Gamma_p$ and $\Gamma_s$ are the overlapping factors of pump and signal light respectively; $h$ is the Planck's constant; $c$ is the light velocity in the vacuum; $A_{cor}$ is the core area of TDF fiber; $l_f$ and $L$ are the length of TDF and resonant cavity respectively; $\tau_f$ is the lifetime of the upper laser level; $\tau = 2n_{cor}L/c[-\ln(R_1R_2) + 2\alpha_s L]$ is the cavity photo lifetime, where $R_1$ and $R_2$ are the reflectivities of input fiber Bragg gating (FBG) and output FBG respectively; $\alpha_s$ is the core absorption coefficient of the fiber at the lasing wavelength; $P(t)$ is pump power as a function of time; $n_{cor}$ is the core index of refraction; $A_{cor}$ is the area of the fiber core; $A_{21}\zeta N_2(t)l_f/L$ represents the contribution of the spontaneous emission to signal laser, where $A_{21}$ is spontaneous emission rate, $\zeta$ is the ratio factor between signal laser and the spontaneous emission.

According to the McCumber formula,[26] we can obtain

$$\frac{f_{up}}{f_{lp}} = \frac{\sigma_e(\lambda_p)}{\sigma_a(\lambda_p)}, \quad \frac{f_{us}}{f_{ls}} = \frac{\sigma_e(\lambda_s)}{\sigma_a(\lambda_s)}, \quad (5)$$

where $\sigma_a(\lambda_p) = f_{lp}\sigma_p$ and $\sigma_e(\lambda_p)$ represent the absorption and emission cross sections at pump wavelength respectively; $\sigma_a(\lambda_s)$ and $\sigma_e(\lambda_s) = f_{us}\sigma_s$ represent the absorption and emission cross sections at laser wavelength, respectively. We assume $\chi_p$=1+$f_{up}$/ $f_{lp}$, $\chi_s$=1+$f_{ls}$/ $f_{us}$, and $N_1(t) = N_0$–$N_2(t)$. Substituting them into Eqs. (2) and (4), we can obtain

$$\frac{dN_2(t)}{dt} = \frac{P(t)}{A_{cor}h\nu_p}\Gamma_p\sigma_a(\lambda_p)[N_0 - \chi_p N_2(t)] - \frac{c}{n_{cor}}\Gamma_s\sigma_e(\lambda_s)[N_0 - \chi_s N_2(t)]\Phi(t) - \frac{N_2(t)}{\tau_f}, \quad (6)$$

$$\frac{\mathrm{d}\Phi(t)}{\mathrm{d}t} = \frac{l_\mathrm{f} c}{L n_\mathrm{cor}} \Gamma_\mathrm{s} \sigma_\mathrm{e}(\lambda_\mathrm{s})[N_0 - \chi_\mathrm{s} N_2(t)]\Phi(t) + \frac{l_\mathrm{f}}{L} A_{21} \zeta N_2(t) - \frac{\Phi(t)}{\tau_0}. \quad (7)$$

Compared with the lifetime of the upper laser level, the width of the pump pulse can be neglected, so it is likely that the resonant cavity starts to oscillate and the action of pump pulse is over. In order to investigate in detail the kinetics of laser oscillation, the process is divided into two stages in a pump period. Assuming that the width of pump pulse is $t_\mathrm{p}$, when $t \in (0, t_\mathrm{p}]$, the process is defined as the energy storage stage, the population inversion of $^3\mathrm{H}_6 \rightarrow {}^3\mathrm{F}_4$ energy level is achieved in this process. When $t > t_\mathrm{p}$, the stored energy will be released, and the output laser pulse is built-up, so this process is defined as energy release stage. In the energy storage stage, the population inversion from $^3\mathrm{H}_6$ to $^3\mathrm{H}_4$ is achieved in the case of pump pulse action, although a part of population is consumed by spontaneous and stimulated emission at the level $^3\mathrm{H}_4$, it is negligible compared with the inversion population. Therefore, by solving the differential equations, we can obtain

$$N_2(t) = \frac{N_0}{\chi_\mathrm{p}} \left\{ 1 - \exp\left[ - \int_0^t \frac{\Gamma_\mathrm{p} \sigma_\mathrm{a}(\lambda_\mathrm{p}) P(\tau)}{A_\mathrm{cor} h \nu_\mathrm{p}} \mathrm{d}\tau \right] \right\}. \quad (8)$$

From Eq. (8), we can see that when $t = t_\mathrm{p}$, the upper level population $N_2(t)$ reaches maximum $N_{2\max}$. At the threshold of the population inversion of $^3\mathrm{H}_4$ ($N_{2\mathrm{th}}$), the variation of cavity photon density $\mathrm{d}\Phi/\mathrm{d}t = 0$. In addition, owing to the number of ions consumed by spontaneous and stimulated absorption being $\ll N_2(t)$, the threshold of population inversion at the $^3\mathrm{H}_4$ level is described by $N_{2\mathrm{th}} = n_\mathrm{cor} L / c \Gamma_\mathrm{s} \tau_0 l \sigma_\mathrm{e}(\lambda_\mathrm{s})$. Assuming $N_{2\mathrm{th}} = N_{2\max}$, we can obtain the threshold of pump energy, which is given by

$$E_\mathrm{th} = \frac{A_\mathrm{cor} h \nu_\mathrm{p}}{\Gamma_\mathrm{p} \sigma_\mathrm{a}(\lambda_\mathrm{p})} \ln\left( \frac{N_0}{N_0 - \chi_P N_{2\mathrm{th}}} \right). \quad (9)$$

From Eq. (9), we can see that the threshold of pump energy is related to the pump wavelength and core diameter of TDF. When the pump wavelength is longer, the threshold is lower; and the core diameter of TDF is smaller, the threshold is also lower.

In the energy release stage, the population of the upper level begins to decrease. Compared with the number of ions consumed by stimulated emission, the number of ions consumed by spontaneous emission is negligible, and the laser pulses are formed in this process. Neglecting the influences of spontaneous and stimulated absorption, Equations (2) and (4) can be simplified. Assuming $t_0$ to be the beginning time of cavity oscillation, the $\Phi(t)$ can be obtained by solving Eqs. (2) and (4), and the expression is given by

$$\Phi(t) - \Phi(t_0) = N_2(t_0) - N_2(t) - N_{2\mathrm{th}} \ln \frac{N_2(t_0)}{N_2(t)}, \quad (10)$$

where $N_2(t_0)$ and $\Phi(t_0)$ are the cavity photon density and upper level population density at the beginning time of cavity oscillation, respectively. Owing to $\Phi(t_0) \ll \Phi(t)$ and $N_2(t_0) \approx N_{2\max}$, equation (9) can be approximately expressed as

$$\Phi(t) \approx N_{2\max} - N_2(t) - N_{2\mathrm{th}} \ln \frac{N_{2\max}}{N_2(t)}. \quad (11)$$

From Eq. (11), it is easy to find that the cavity photon density $\Phi(t)$ can reach up to a maximum, $\Phi_\mathrm{max}$, when $N_2(t) = N_{2\mathrm{th}}$. Assuming $\psi = N_{2\max}/N_{2\mathrm{th}}$, we can have

$$\frac{\Phi_\mathrm{max}}{N_{2\max}} = \varphi(\psi) = \frac{\psi - 1 - \ln\psi}{\psi}, \quad (12)$$

where $\psi$ is defined as that pump intensity factor, and $\varphi$ ($\psi$) is defined as the extraction efficiency of the laser peak power from the stored cavity energy.

Although the laser pulse generated by stimulated emission will consume most of the upper-level population, a part of population remains in the upper-level after a laser pulse, and $N_{2\mathrm{r}}$ is used to describe the residual population. The expression of $N_{2\mathrm{r}}$ cannot be explicitly given, but it is reasonable to assume that the cavity photon number is approximately zero when the upper-level population is consumed into $N_{2\mathrm{r}}$. Assuming $N_2(t) = N_{2\mathrm{r}}$, equation (11) can be written as

$$\frac{1}{\psi} \ln \frac{N_{2\mathrm{r}}}{N_{2\max}} = \frac{N_{2\mathrm{r}}}{N_{2\max}} - 1. \quad (13)$$

In order to describe the extraction efficiency of an entire laser pulse from the maximum upper-level population $N_{2\max}$, the pulse extraction efficiency ($\eta$) is introduced, and expressed as

$$\eta = \frac{N_{2\max} - N_{2\mathrm{r}}}{N_{2\max}} = 1 - \frac{N_{2\mathrm{r}}}{N_{2\max}}. \quad (14)$$

Substituting Eq. (14) into Eq. (13), the relationship between $\eta$ and $\psi$ is given by

$$\frac{1}{\psi} \ln(1 - \eta) + \eta = 0. \quad (15)$$

Considering the conventional model of coupled rate equations, the output power $P$ is given by[24]

$$P(t) = \frac{\Phi(t) c}{2 n_\mathrm{cor}} \ln\left( \frac{1}{R_1 R_2} \right) A_\mathrm{cor} h \nu_\mathrm{s}. \quad (16)$$

Typical parameters corresponding to a practical laser of gain-switched TDF are employed as follows: $\lambda_\mathrm{p} = 1558$ nm, $\lambda_\mathrm{s} = 1940$ nm, $\sigma_\mathrm{a}$ ($\lambda_\mathrm{p}$), $\sigma_\mathrm{e}$ ($\lambda_\mathrm{p}$), $\sigma_\mathrm{a}$ ($\lambda_\mathrm{s}$), and $\sigma_\mathrm{e}$ ($\lambda_\mathrm{s}$) (see Ref. [27]), $\tau_\mathrm{f} = 334.7$ μs, $R_1 = 0.99$, $R_2 = 0.8$, $\Gamma_\mathrm{s} = 0.8$, $\Gamma_\mathrm{p} = 0.8$, $N_0 = 2$ wt%, $h = 6.6261 \times 10^{-34}$ J·s, $t_\mathrm{p} = 100$ ns, $l_\mathrm{f} = 20$ cm, $A_\mathrm{cor} = 3.12 \times 10^{-11}$ m$^2$, and $n_\mathrm{cor} = 1.456$. Figure 1 shows the variations of upper-level population density and the cavity photon density at different pump powers. One can see that the upper-level population density sharply increases under

a pump pulse action, and the growth rate of upper-level population increases as pump power increases. Due to the long lifetime of the upper laser level (hundreds of microseconds), the number of ions consumed by spontaneous emission is negligible, so the number of upper level population can be approximately considered as a constant at a certain time. With the increase in the stimulated emission, the upper-level population begins to decrease sharply, and the laser pulse is generated. At a higher pump power, the upper-level population sharply reaches a maximum within a pump pulse width, and the stimulated emission occurs quickly. At remaining pump time, the upper level population exceeds the threshold population $N_{2\mathrm{th}}$ ($\approx 4.65\times10^{24}/\mathrm{m}^3$), and the other stimulated emission will occur. As a result, the output laser pulse will produce a mutipulse phenomenon when the upper-level population arrives at a value, 4–5 times $N_{2\mathrm{th}}$ (see Fig. 2).

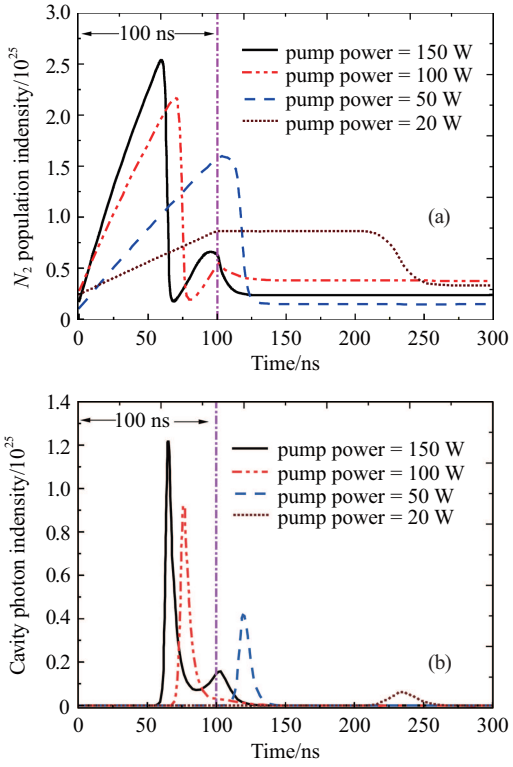



**Fig. 1.** (color online) Calculated variations of $^3F_4$ level population density and the cavity photon density under a pump pulse action at different pump powers.

The peak power extraction efficiency and pulse extraction efficiency are plotted with respect to the pump intensity factor in Fig. 2. When pump intensity factor $\psi = 5$, the peak power extraction efficiency is 48%, which means 48% upper-level population is consumed by the laser peak power, and the rest of population is consumed by the front edge and trailing edge of laser pulse. The bigger the conversion ratio between $N_{2\max}$ and $\Phi_{\max}$, the higher the output laser peak power is and the shorter the width of laser pulse is. Also when pump intensity factor $\psi = 5$, the pulse extraction efficiency $\eta$ is approximately 1, which means that the stored energy is almost exhausted. There are two ways to improve the pulse extraction efficiency $\eta$. One is to improve the pump power, and the other is to reduce the cavity loss, especially the useless loss.

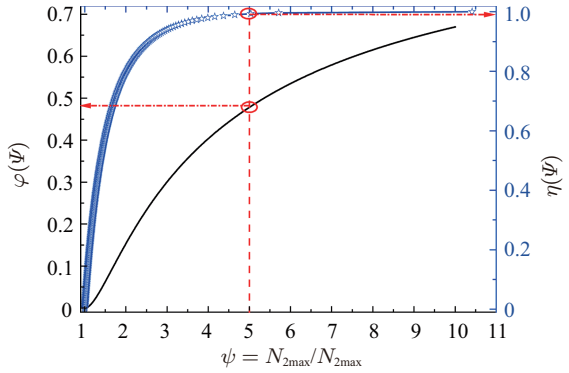



**Fig. 2.** (color online) Variations of peak power extraction efficiency and pulse extraction efficiency with pump intensity factor.

## 3. Experiments and results

The experimental setup is shown in Fig. 3. The pump source for the gain-switched Tm-doped fiber laser consists of a modulated diode at 1.558-μm wavelength and two stages of amplification. A single mode (SM) 1.558-μm diode laser (JDSU CQF935/6636.5) is selected as a seed laser, which is driven by a modulated circuit, resulting in the generation of 200 ns–5 μs pulse duration and 3 kHz–30 kHz modulated repetition rate square shape. An isolator between the seed laser and pulse amplifier protects the diode laser from damaging by backreflected light, such as amplifier spontaneous emission (ASE) and simulated Brillouin scattering (SBS). The 10 μm/125 μm single mode (SM) erbium-doped fiber (EDF) is selected as the gain fiber, the peak absorption coefficient near 980 nm is higher than 15 dB/m. and an about 80-cm-long active fiber is used in experiment. The optimal EDF lengths of the 1st and 2nd stages are 0.8 m and 1.2 m, respectively.

The gain-switched cavity consists of a segment of $Tm^{3+}$-doped double clad fiber (DCF) which is spliced between two FBGs to form the laser resonator. The TDF is a commercially available DCF (CorActive Inc.) with core diameter 6±1 μm, inner clad diameter 125±3 μm, core NA about 0.23±0.02, and clad NA $> 0.45$. The $Tm^{3+}$ ion doping concentration is $\sim 2$ wt%, and an approximate 19-cm long TDF is used in the experiment. The FBGs are inscribed by the phase mask method using the UV lasers in a passive fiber which is matched to the Tm-doped fiber. The input coupler FBG1 has a high reflectivity ($R \sim 94\%$) near 1940 nm and a bandwidth of ~0.4 nm. The FBG2 (serving as the output coupler) has partial reflectivity ($R \sim 65\%$) near 1940 nm. At the output end, a dichroic mirror is used to separate the 1940-nm laser pulse from the 1558-nm pump pulse.

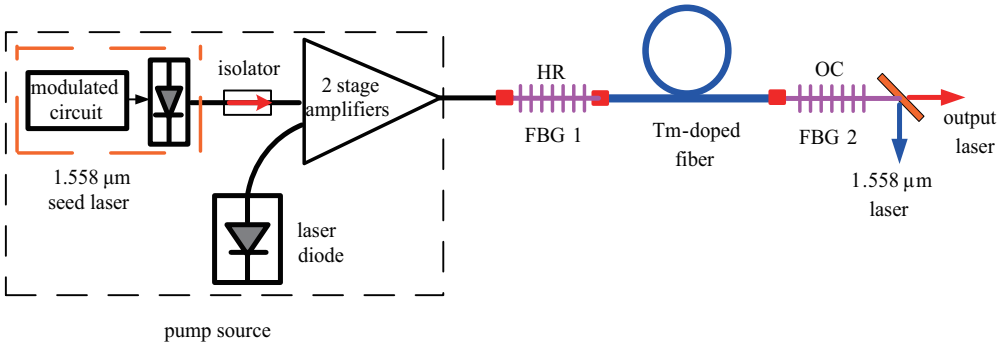



**Fig. 3.** (color online) Experimental setup of the gain-switched TDF laser.

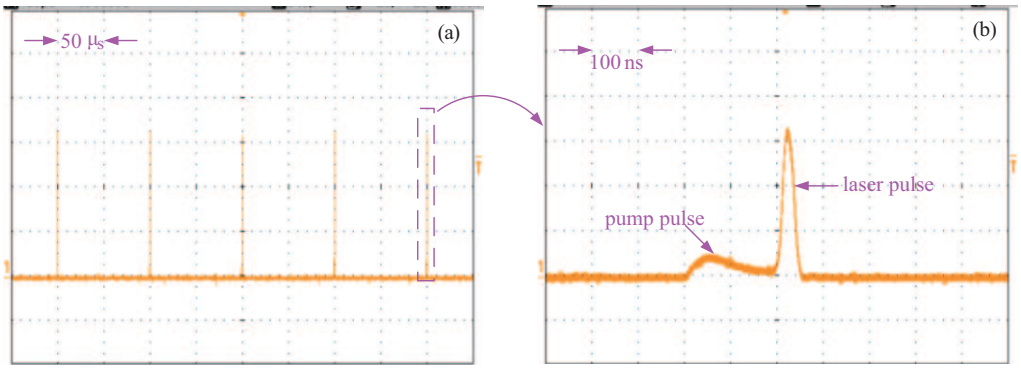



**Fig. 4.** (color online) Output laser pulse of the 1.558-μm pumped gain-switched TDF laser at a repetition rate of 10 kHz.

The laser pulse is detected by an InGaAs photodiode and recorded by a 350-MHz digital oscilloscope (wavejet332, Lecroy). Figure 4 shows the output pulse of the gain-switched TDF laser at a 10-kHz repetition rate. In Fig. 5(a), the output pulse cluster is stable and the effect of amplitude variation is negligible. Figure 4(b) shows the magnified curve of the pulse (dotted line) in Fig. 4(a). One can find that the front edge of laser pulse overlaps with the trailing edge of the pump pulse. Using parameters for this laser setup, the numerical model predicts the pump energy threshold and stable output power as a function of incident pump power, and the pump energy threshold is about 0.27 μJ.

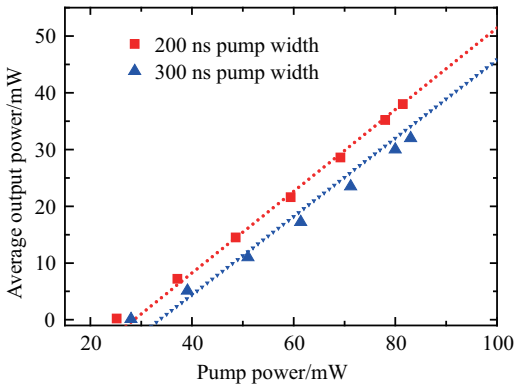



**Fig. 5.** (color online) Plots of output laser power versus incident pump power at pump widths of 200 ns and 300 ns.

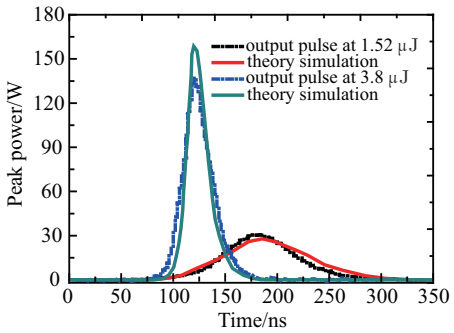



**Fig. 6.** (color online) Comparisons between the simulated and experimental pulse outputs at 1.52 μJ and 3.8 μJ.

Figure 5 shows the plots of output power versus incident pump power for 200-ns and 300-ns pump widths. The experimental results are in good agreement with theoretical prediction data in which taken into account are the fusion loss and coupler loss between the FBGs and standard single mode fiber. The output pulses and theory simulation are compared in Fig. 6 at 200-ns pump width. The experimental output pulse energies are 1.52 μJ and 3.8 μJ, and the pulse width are 50.2 ns and 30 ns, respectively. The theoretical output pulse shapes are also calculated under the corresponding conditions, although some errors exist between the experiments and the simulation, overall the numerical model well describes the operating behaviors and output characteristics of stable in-band pumped gain-switched TDF lasers.

## 4. Conclusions

In this paper, the theoretical rate equation model of an in-band pumped gain-switched TDF laser is built. By solving the rate equation, the analytical formulations of pump energy threshold, peak power extraction efficiency, and pulse extraction efficiency are obtained, and the interaction process between the pump pulse and the laser pulse is also discussed. The practical example of the stable in-pumped gain-switched TDF laser is used to verify the present theoretical model, and the experimental data are in very good agreement with theoretical results.

## References


[1] Pierce M C, Jackson S D, Dickinson M R and King T A 1999 *Lasers Surg. Med.* **25** 407
[2] Jackson S D and Lauto A 2002 *Lasers Surg. Med.* **30** 184
[3] Frid N M 2005 *Lasers, Surg. Med.* **36** 52
[4] Frid N M 2005 *Lasers, Surg. Med.* **37** 53
[5] Daly J G 2001 *Proc. SPIE* **94** 1419
[6] Yao B Q, He W J, Wang Y Z, Zhang X B and Li Y F 2004 *Chin. Phys. Lett.* **21** 2182
[7] Shen Y J, Yao B Q, Duan X M, Zhu G L, Ju Y L and Wang Y Z 2012 *Opt. Lett.* **17** 3558
[8] Zhang X L, Ju Y L and Wang Y Z 2005 *Opt. Express* **13** 4056
[9] He W J, Yao B Q, Ju Y L and Wang Y Z 2006 *Opt. Express* **14** 11653
[10] Fan S, Zhang X, Wang Q, Li S, Ding S and Su F 2006 *Opt. Commun.* **266** 620
[11] Moshe I, Jackel S and Meir A 2003 *Opt. Lett.* **28** 807
[12] Marc E and Stuart D J 2006 *Opt. Lett.* **32** 1672
[13] Marc E 2007 *Opt. Lett.* **32** 1056
[14] Marc E and Stuart D J 2008 *Opt. Lett.* **33** 1044
[15] Dickinson B C, Jackson S D and King T A 2000 *Opt. Commun.* **182** 199
[16] Jackson S D and King T A 2002 *IEEE J. Quantum Electron.* **34** 779
[17] ZhangY J, Yao B Q , Ju Y L and Wang Y Z 2005 *Opt. Express* **13** 1085
[18] Jiang M and Tayebati P 2007 *Opt. Lett.* **32** 1797
[19] Nakagami H, Araki S and Sakata H 2011 *Laser Phys. Lett.* **8** 301
[20] Nikita S, Alex H, Shayne B and John H 2011 *Opt. Express* **16** 14949
[21] Ding J W, Samson B, Cater A, Wang C C and Tankala K 2011 *Proc. SPIE* **7914** 79140X-1
[22] Wang F, Shen D Y, Chen H, Fan D Y and Liu Q S 2009 *Opt. Rev.* **18** 360
[23] Zhang G W 1995 *Laser Technol.* **19** 129 (in Chinese)
[24] Koechner W 2006 *Solid-State Laser Engineering*, 6th edn. (New York: Springer)
[25] Yao J Q and Zhang D G 2007 *Solid-State Laser and Nonlinear Optical Frequency Transformation* (Beijing: Science Press)
[26] McCumber E 1964 *Phys. Rev.* **134** A299
[27] Soren D A and Jorn H P 2006 *Opt. Express* **14** 50